Biosensors and Bioelectronics 175 (2021) 112833

Contents lists available at ScienceDirect

Biosensors and Bioelectronics

journal homepage: http://www.elsevier.com/locate/bios

Unidirectional intercellular communication on a microfluidic chip

Guocheng Fang [a], Hongxu Lu [a,*], Hamidreza Aboulkheyr Es [b], Dejiang Wang [a], Yuan Liu [a], Majid Ebrahimi Warkiani [b], Gungun Lin [a], Dayong Jin [a,c,**]

[a] Institute for Biomedical Materials and Devices, School of Mathematical and Physical Sciences, University of Technology Sydney, Broadway Ultimo, Sydney, NSW, 2007, Australia

[b] School of Biomedical Engineering, University of Technology Sydney, Broadway Ultimo, Sydney, NSW, 2007, Australia

[c] UTS-SUSTech Joint Research Centre for Biomedical Materials & Devices, Department of Biomedical Engineering, Southern University of Science and Technology, Shenzhen, China

ARTICLE INFO

Keywords:
Intercellular communications
Microfluidic chips
Cancer-associated fibroblasts
Mesenchymal stem cells

ABSTRACT

Cell co-culture serves as a standard method to study intercellular communication. However, random diffusion of signal molecules during co-culture may arouse crosstalk among different types of cells and hide directive signal-target responses. Here, a microfluidic chip is proposed to study unidirectional intercellular communication by spatially controlling the flow of the signal molecules. The chip contains two separated chambers connected by two channels where the culture media flows oppositely. A zigzag signal-blocking channel is designed to study the function of a specific signal. The chip is applied to study the unidirectional communication between tumor cells and stromal cells. It shows that the expression of α-smooth muscle actin (a marker of cancer-associated fibroblast (CAF)) of both MRC-5 fibroblasts and mesenchymal stem cells can be up-regulated only by the secreta from invasive MDA-MB-231 cells, but not from non-invasive MCF-7 cells. The proliferation of the tumor cells can be improved by the stromal cells. Moreover, transforming growth factor beta 1 is found as one of the main factors for CAF transformation via the signal-blocking function. The chip achieves unidirectional cell communication along X-axis, signal concentration gradient along Y-axis and 3D cell culture along Z-axis, which provides a useful tool for cell communication studies.

1. Introduction

Intercellular communication is crucial to coordinate cell behaviors and maintain cell functions in multicellular organisms (Kholodenko 2006). Cells communicate by means of signal molecules through Signal-Target-Response activities (Telleen 2018). These signals may include proteins, small peptides, amino acids, nucleotides, fatty acid derivatives, and even dissolved gases such as nitric oxide and carbon monoxide. Most of these signal molecules are secreted from the signaling cell and interact with the receptors in the target cell to trigger a response that alters the behavior of the target cell (Alberts et al., 2002).

There are two types of communications between cells: the direct communication between physically connected cells via gap junctions and the indirect communication between non-contacted cells via paracrine and hormonal secretion (Telleen 2018). To study cell communications, cells are isolated from organisms and cultured *in vitro* so that specific signals can be tested and cellular responses can be measured (Neitzel and Rasband). Cell co-culture has been developed as a standard approach to study the communication between different types of cells. The current methods of cell co-culture can be divided into three major categories, as shown in Fig. 1A. The contact co-culture mixes different types of cells and cultures in the same culture vessel (Fig. 1A–i). It offers physical contact between the cells. With this method, the population morphology of the cell may be lost, and it is difficult to identify whether the target cell receives signals via gap junctions or other receptors in the cell.

The semi-separate co-culture restricts cells in a separated space while enables commutation of signals in the culture media (Fig. 1A-ii). The most frequently used device is the cell culture inserts hanging in multi-well plates. Cells grow on the permeable membrane of the inserts, separating from another type of cells grow in multi-well plates. At the same time, the signals from both cell types can be exchanged during

* Corresponding author.
** Corresponding author. Institute for Biomedical Materials and Devices, School of Mathematical and Physical Sciences, University of Technology Sydney, Broadway Ultimo, Sydney, NSW, 2007, Australia.
E-mail addresses: Hongxu.Lu@uts.edu.au (H. Lu), Dayong.Jin@uts.edu.au (D. Jin).

https://doi.org/10.1016/j.bios.2020.112833
Received 9 September 2020; Received in revised form 29 October 2020; Accepted 17 November 2020
Available online 24 November 2020

culture. As the cells in the inserts cannot be visualized in a real-time fashion, interactive co-culture plates have also been developed with two horizontally arranged chambers that are separated by a permeable membrane (Moutinho et al., 2017; Shimasaki et al., 2018). Microfluidic technology has been rapidly developed in the past decades and become a promising approach in biomedical research (Lin et al. 2019, 2020; Truong et al., 2019b). The miniaturize microfluidic chips offers precise control of fluid, low consumption of reagents, high efficiency of analysis, and high throughput capacity (Dorayappan et al., 2019; Lin et al., 2020; Shim et al., 2019). Various chip-based methods have been applied to study cell communications (Jeong et al., 2016; Vu et al., 2017; Yu et al., 2019; Zervantonakis et al., 2012). Generally, two or more chambers are fabricated on a chip; the chambers are semi-separated using physical barriers, such as flow channels, permeable membrane and hydrogels, which only allow the exchange of signal molecules but not cells (Jeong et al., 2020; Jiang et al., 2016; Lin et al. 2019, 2020; Vu et al., 2017). For example, Zervantonakis *et al.* fabricated a microfluidic chip with three channels separated by physical barriers to study the communication of tumor cells and endothelial cells (Zervantonakis et al., 2012). The tumor cells were mixed in 3D extracellular matrix (ECM) hydrogel in the middle channel, and endothelial cells were monolayer cultured in one of the side channels. Jeong et al. co-cultured tumor spheroids and fibroblasts in a collagen matrix-incorporated microfluidic chip to study the interaction between different cell types (Jeong et al., 2016). Recently, Yu *et al.* designed a kind of culturing modules that can be reconfigured together, holding potentials to be applied to study the communication of unlimited types of cells (Yu et al., 2019). However, in the above methods, the exchange of signal molecules relies on passive diffusion, which cannot avoid the crosstalk of signals from both different cell types; the influenced and radically changed cells may, in turn, affect the secretor cells (Lee et al., 2018). It may conceal the truth underlying mechanisms in intracellular communications.

Transferring of conditioned medium from one cell type to another provides a solution to avoid the crosstalk and interference of communication signals (Fig. 1A-iii). The advantages of conditioned media include its simplicity in allowing for the detection of any soluble factor-related effects, along with the potential for subsequent identification of these factors in the co-culture media (Bogdanowicz and Lu 2013). However, as the conditioned media are collected and then transferred, the signals may suffer a loss of bioactivities and compromised nutrient supply.

In this study, we report a microfluidic-chip-based cell co-culture method to study unidirectional intercellular communication. The chip consists of two separated chambers and two surrounded medium channels. Two types of cells mixed in Matrigel can be loaded into different chambers, respectively. The flow directions of the medium in the two channels were set as the opposite. The signal molecules secreted from each chamber can enter the channel and flow to the opposite chamber. Thus, we can monitor the unidirectional communication between the cells due to the flow control. Besides, due to the matter of diffusion, there will be a concentration gradient of the signal molecules vertically. Moreover, another advantage of the unidirectional chip is the real-time analysis of the functional signals with the signal-blocking inlet. For instance, when one wants to know the function of Signal I, the related blocking agents could be introduced in the channels. The agents will interact with the Signal I in the zigzag mixing channel, then block their functions before reaching another cell culture chamber.

Amongst various cell types within the tumor microenvironment, cancer-associated fibroblasts (CAFs) are in abundance, serving to modulate the behaviors of cancer cells in progression (Aboulkheyr Es et al., 2020; Cirri and Chiarugi 2011; Kalluri 2016; Kalluri and Zeisberg 2006; Saini et al., 2020). Little is yet known about how cancer cells transform normal stromal cells into CAFs (Mitra et al., 2012). It is not clear whether direct contact with cancer cells is necessary for the transformation of CAFs. Several growth factors and cytokines have been reported to transform normal stromal cells into CAFs (Kalluri 2016; Kalluri and Zeisberg 2006). At the same time, CAFs also secret various signal molecules to regulate cancer cells. With the previously reported methods, it is challenging to reveal the unidirectional influence from one cell type to another. Thus, a reductionist approach is desired to study the

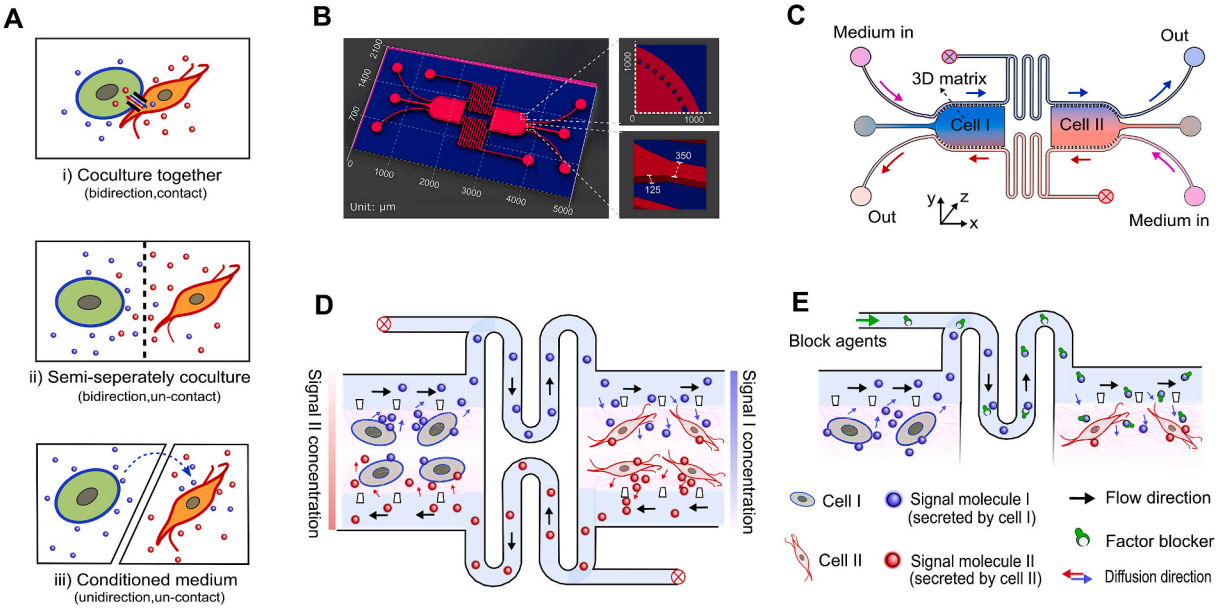

Fig. 1. The co-culture approaches for intercellular communication studies (A) and the schematic of the unidirectional microfluidic chip (B–E). (A) The co-culture approaches to study the cell communication: i) Cell co-culture in the same vessel offers the bidirectional and contact communication; ii) Semi-separated co-culture offers bidirectional and noncontact communication; iii) Transferring the conditioned medium offers unidirectional and noncontact communication. (B) The design of the unidirectional microfluidic chip. (C) The schematic is showing how the chip works during co-culture. Different types of cells are cultured in the left and right chambers with Matrigel, respectively. The black arrows show the flow directions of the cell culture media in the channels. The signal-blocking inlets are close unless a specific signal is being neutralized. (D) Detailed working mechanisms of the unidirectional communication chip. Due to the matter of diffusion, there is a concentration gradient of signal molecules along Y-axis. (E) Detailed working mechanisms for signal-blocking studies.

unidirectional interaction between stromal cells and tumor cells. In this work, we used the microfluidic chip to study the unidirectional communication of breast cancer cells (invasive MDA-MB-231 and non-invasive MCF-7 cells) and stromal cells (MRC-5 fibroblasts and mesenchymal stem cells (MSCs)). We observed the growth and spheroid formation of cancer cells and the transformation of MRC-5 and MSCs into myofibroblasts-like cells. We also used an antibody against transforming growth factor beta 1 (TGF-β1) to demonstrate the function of the signal blocking inlet as TGF-β1 secreted from cancer cells have been reported to induce the formation of CAFs.

2. Materials and methods

2.1. Chip fabrication and process

The design of the microfluidic device was shown in Fig. 1B and Fig. S1. The device was fabricated with polydimethylsiloxane (PDMS) (Sylgard® 184, Sigma Aldrich) by replicate molding on a SU8-2075 silicon master. Firstly, a 4-inch silicon wafer was cleaned using isopropanol and then heated in an oven at 150 °C for 20 min. The SU8-2075 was spin-coated on the wafer at 1250 rpm for 30 s, which was followed by soft bake at 65 °C for 5 min and 95 °C for 25 min. The thickness of the SU8-2075 layer was around 125 μm. Then the SU8-2075 wafer was exposed under a laser scanning lithographer (μPG 101, Heidelberg Instruments, Germany) to generate patterns designed with CAD software. After the exposure, the wafer was incubated at 65 °C for 5 min and 95 °C for 30 min followed by a development process for 30 min at room temperature. Finally, the SU8-2075 master was treated with a process called hard bake at 150 °C for 30 min. Once the master was prepared, PDMS was mixed thoroughly with the curing agent at a weight ratio of 10:1. Then the PDMS was poured on the master mold and heated in the oven at 80 °C for 2 h. After the solidification, the PDMS was gently peeled off from the mold and trimmed with a scalpel. Then the inlets and outlets on the PDMS were punched with an Ø1mm puncher. The thickness of the PDMS was 5 mm. Finally, the PDMS piece was firmly bound to 1.2-mm thick glass slides after plasma treatment for 1min, which was followed by heating at 80 °C for 2 h. Before cell seeding, the chips were laid aside for 24 h to reduce the hydrophilicity induced by the plasma treatment.

2.2. Cell culture and cell seeding

Human breast carcinoma cell, MDA-MB-231 and MCF-7, and lung fibroblasts MRC-5 from Australia Cell Bank were cultured with DMEM medium with 10% fetal bovine serum (FBS) and 100 U/mL penicillin/streptomycin (Life Technologies, Australia) in 25 mm^2 flasks. Human bone marrow mesenchymal stem cells (MSCs) were purchased from Merck Australia and cultured with Stemline® mesenchymal stem cell expansion medium (Sigma Aldrich, Australia) in 25 mm^2 flasks. The cells were incubated in an incubator with 5% CO_2 at 37 °C and passaged once they reached 70–80% confluence.

To collect cell suspension, the cells were treated with Trypsin-EDTA solution for 3 min, followed by centrifugation for 5 min at 500×*g*. After removing the supernatant, the cells were re-suspended in 75 μL Matrigel (Corning, USA) by pipetting at a density of 1×10^6 cells mL^{-1}. The 75 μL Matrigel allowed loading of three chambers, which means that a chip with two chambers only needs 50 μL Matrigel. The whole process was operated on the ice, avoiding the gelation of the Matrigel. The chips were sterilized under UV for 30 min before the cell seeding. Then the Matrigel containing cells were loaded gently into the culture chambers in the middle of the chip with 1 mL syringes. Due to the surface tension effect around the barriers, the Matrigel could only fulfil the chambers but without any leakage into the medium flow channels. To ensure the uniform distribution of cells in the chamber, we should mix the cells with Matrigel well. The cell distribution was mapped and shown in Fig. S3. After the cell seeding, the chips were put in the incubator for 30 min to allow gelation of the Matrigel. The chip was then connected to 3 mL medium containing syringes through polyethylene tubing (outer Ø of 1 mm and inner Ø of 0.8 mm). A syringe pump (11 Elite, Harvard Apparatus) was used to control the injection volume at 1 μL min^{-1}, which resulted in a flow speed in the channels at 50 μm s^{-1}. The flow directions were set opposite to allow unidirectional communication of signal molecules and nutrition supply.

2.3. Signal molecule diffusion in the chamber

To quantify the effective transfer of secreted signal molecules in the Matrigel, we used three different fluorophores to simulate the diffusion of signal molecules: Cy5-labelled anti-rabbit antibody, doxorubicin and poly (N-(2-hydroxypropyl)methacrylamide) (PHPMA)-based block copolymeric micelles. They were dissolved in phosphate-buffered saline (PBS) with the concentration of 10 ng mL^{-1}, 30 μg mL^{-1}, and 100 μg mL^{-1}, respectively. Then they were injected in the flow channel. The opposite channel was injected with pure PBS. The flow rate was set around 50 μm s^{-1}. During the perfusion, the chip was placed in the CO_2 incubator. After the perfusion, the fluorescence was investigated under an Olympus FV1200 laser scanning confocal microscopy.

2.4. Characterization of cell responses

To quantify the MDA-MB-231 and MCF-7 cells on the chip, we used the Hoechst 33342 and Orange CMRA Cell Tracker (Life technologies) to stain cell nuclei and membrane, respectively. Firstly, the cells were fixed with 100 μL 4% phosphate-buffered paraformaldehyde for 1 h on the chip. Then the staining solution of Hoechst 33342 (10 ng mL^{-1}) and Orange CMRA CellTracker (1:1000 dilution) in PBS was perfused for 3 h. PBS was used to wash the chip to remove unbound dyes. The cells were then observed under the confocal microscopy.

To evaluate the induction of CAF, we measured the expression of α-smooth muscle actin (α-SMA) by immunofluorescence staining. The cells were first fixed with 4% paraformaldehyde on the chip for 1hr. To accelerate the staining and washing process, we then used a scalpel to separate the PDMS piece from the glass slide. The Matrigel and cells were kept in the PDMS chamber, and we directly stained the cells on the PDMS. The cells in the Matrigel was treated with 1% Triton X-100 for 1 h, followed by washing with PBS three times. Then cells were blocked with 5% bovine serum albumin (BSA)/PBS solution at 37 °C for 1 h before the anti α-SMA antibody (Sigma Aldrich) (1:100 dilution in 0.1% BSA/PBS) was applied to the cells for 1 h. After washing with PBS thrice, the cells were immersed in the Cy5-labelled second antibody solution (1:100 dilution in 0.1% BSA/PBS) at 37 °C for 1 h. The antibody was dissolved in the 0.1% BAS PBS solution. The cells were then observed under microscopy.

2.5. Fluorescence measurement and data process

The image was captured under a laser scanning confocal microscope (FV1200, Olympus, Japan). The settings for the dyes: Hoechst 33342, excitation at ~350 nm and emission at ~461 nm; CellTracker excitation at ~548 nm and emission at ~576 nm; Cy5-labelled second antibody, excitation at ~650 nm and emission at ~670 nm. For the size calculation of the spheroids, the bright-field images were processed by Adobe Illustrator CS6 to enhance the contrast of the spheroids. Then the images were processed by ImageJ to automatically recognize the spheroids and calculate the size (area, perimeter, etc.). For the fluorescent images, we measured the mean grey value of the images under the same threshold in ImageJ and then calculate the ratio of α-SMA to cell nuclei.

2.6. Blocking of signal molecules on the chip

We used anti TGF-β1 antibody (Novus Biologicals, USA) to block the TGF-β1 secreted from the cancer cells. The cancer cells and

mesenchymal stem cells were seeded in the left and right chambers, respectively. After the gelation of the Matrigel, we started to perfuse the chambers with cell culture medium from the medium inlet. A solution containing 10 ng mL^{-1} anti TGF-β1 antibodies (diluted in 0.1% BSA/PBS) was injected to blocking agent inlet. After three days' culture, the cells were fixed and stained as described above.

2.7. Statistical analysis

All the data were presented by means ± standard deviation. Two-tailed student's tests were used to reveal the statistical difference between the groups with OriginLab 8.0. A p value less than 0.05 was considered as significant difference ($p < 0.05$).

3. Results and discussion

3.1. Design concept of the unidirectional-communication chip

The microfluidic chip was fabricated with PDMS. The chip consists of two separated half-ellipse-shaped chambers, as shown in Fig. 1B. Each chamber has an inlet, which is used for cell loading. The thickness of the chamber is designed as 125 μm, and the width of the inlet channel is about 350 μm. The chambers are surrounded by two channels of 250 μm width for medium flow. The chambers and channels are semi-separated by physical barriers. The channels also connect the two chambers by a zigzag-shaped part. The detailed design and the gross appearance of the chip are shown in Fig. S1. As shown in Fig. 1C, the two types of cells are mixed in Matrigel separately and then injected into the left and right chambers, respectively. Due to the barriers between the chambers and the channels, the Matrigel will be restrained within the chamber area. Cell culture medium flows in the channels, and the flow directions are opposite, as shown by the black arrows. Due to the Matrigel and the physical barriers, the medium could only flow along the channels. The nutrition and oxygen in the medium can diffuse into the Matrigel through the gap between the barriers. The blocking agent inlets are closed unless we evaluate the function of signal molecules and their targets.

The working mechanism of the unidirectional chip is shown in Fig. 1C. The Signal I secreted by Cells I from the left chamber can diffuse into the medium channel and flow with the medium. When they arrive at the channel around the right chamber, the Signal I molecules will diffuse into the matrix through the gaps between the barriers, and then target Cells II. We could imagine that the closer to the top channel, the larger the concentration of the signal molecules is. It will form a vertical concentration gradient of the Signal I in the right chamber. At the bottom of the right chamber, there is an area containing almost no Signal I molecules. Similarly, Signal II molecules secreted by the Cells II in the right chamber will flow into the left chamber, form a concentration gradient and then work on the Cells I. The flow direction enables the unidirectional communication that the Cells I could only be influenced by the original type of the cells II and thus avoids the interference from the affected Cells II.

The chip can achieve the unidirectional communication of cells along X-axis, the concentration gradient along Y-axis and 3D cell culture along Z-axis. Owning to the nature of the microfluidic device, it can significantly reduce the consumption of cells, medium and reagents as well as facilitate the observation of cell responses. Also, another advantage of our unidirectional chip is the real-time analysis of the functional signals with the signal-blocking inlet, as shown in Fig. 1D. For instance, if we want to know the function of Signal I, the related blocking agents could be introduced in the channels. The agents will interact with the Signal I in the zigzag mixing channel, then block their functions when they reach another cell culture chamber.

3.2. Molecule diffusion on the chip

We used several fluorophores with different sizes to verify the diffusion of signal molecules and the formation of concentration gradients. The experiment was observed under a laser-scanning confocal microscope, as shown in Fig. 2A. The fluorophores dissolved in PBS was introduced into one channel of the Matrigel-loaded chip, and blank PBS was introduced into the opposite channel. The flow directions were set as opposite, and the flowing rate was set about 50 μm s^{-1}. First, we used the Cy5-labelled anti-rabbit antibody, which has a molecule weight of around 150 kDa, as a model of protein diffusion. The diffusion was profiled at 20 min, 6 h and 24 h, respectively, as shown in Fig. 2B. The fluorescence intensity was quantified by ImageJ. We could see that the proteins were mainly distributed in the channel at the beginning of injection. After 6 h, the proteins diffused into the Matrigel towards the opposite channel, and the fluorescence intensity in the middle area reached 20%. The fluorescent curvy showed a slightly concave shape. After 24 h, the fluorescent distribution curve became straight. The fluorescence intensity in the middle area reached around 40%. The fluorescence illustrated the formation of concentration gradient of proteins. The fluorescence distribution in the whole chamber was profiled after 24 h, as shown in Fig. 2C. A 3D illustration of the intensity for the concentration gradient was shown in Fig. 2D.

The diffusion of doxorubicin (molar mass: 543.52 g mol^{-1}) was also investigated with the same method described above. As shown in Fig. 2E, at 20 min, doxorubicin diffused over about 500 μm in the Matrigel. After 6 h, weak fluorescence reached the opposite side of the Matrigel. Differently, the fluorescence intensity near the physical barrier was stronger than that in the flow channel, which means that the doxorubicin accumulated in the edge of the Matrigel. After 24 h, the red fluorescence fulfilled the whole chamber with a concentration gradient. The fluorescence intensity of the middle area reached around 60% of that at the edge.

PHPMA-based micelles have been used as nanocarriers to deliver anticancer agents (Lu et al., 2015). Here, the PHPMA micelles labelled with fluorescence are used to model the diffusion efficiency of nanosized vesicles. The structure of the PHPMA micelle is shown in Fig. 2G. The average size of the micelles was 15 nm measured by dynamic light scattering (Fig. S2). As shown in Fig. 2H, the nanoparticles diffused little into the Matrigel after 20 min. After 6 h, the nanoparticles gradually diffused into the Matrigel. The fluorescence intensity of the middle area reached only around 18% with the intensity curvy being a little concave. After 24 h, the fluorescence near the flow channel was enhanced. However, the fluorescence far away from the flow channel only changed slightly. The intensity curvy became more concave than the beginning. The results show that the distribution of the nanoparticle concentration was also gradient. Compared to the three molecules, the result shows a size-dependent diffusion pattern in the Matrigel, indicating that the chip allows intercellular communication via the molecule diffusion through Matrigel.

3.3. MDA-MB-231 and MCF-7 cells are different to influence stromal cells

The tumor tissue consists of tumor cells and stromal cells, such as the normal fibroblasts, CAFs, vascular cells, and some resident immune cells. The communication between the tumor cells and the stromal cells are critical to regulating tumor cell responses to the treatment. CAF is a heterogeneous population of dynamically varied from mesenchymal cells with functions that are likely different from those of resident fibroblasts (Kalluri 2016; Kalluri and Zeisberg 2006). They are abundant in the tumor, which could help to stimulate the angiogenesis, support the formation, proliferation, and metastasis of the tumor. The origin of CAFs is debated; however, it is commonly believed that they are the communication product of tumor and more than one precursor cells (Shimoda et al., 2010). The normal fibroblasts are an attractive

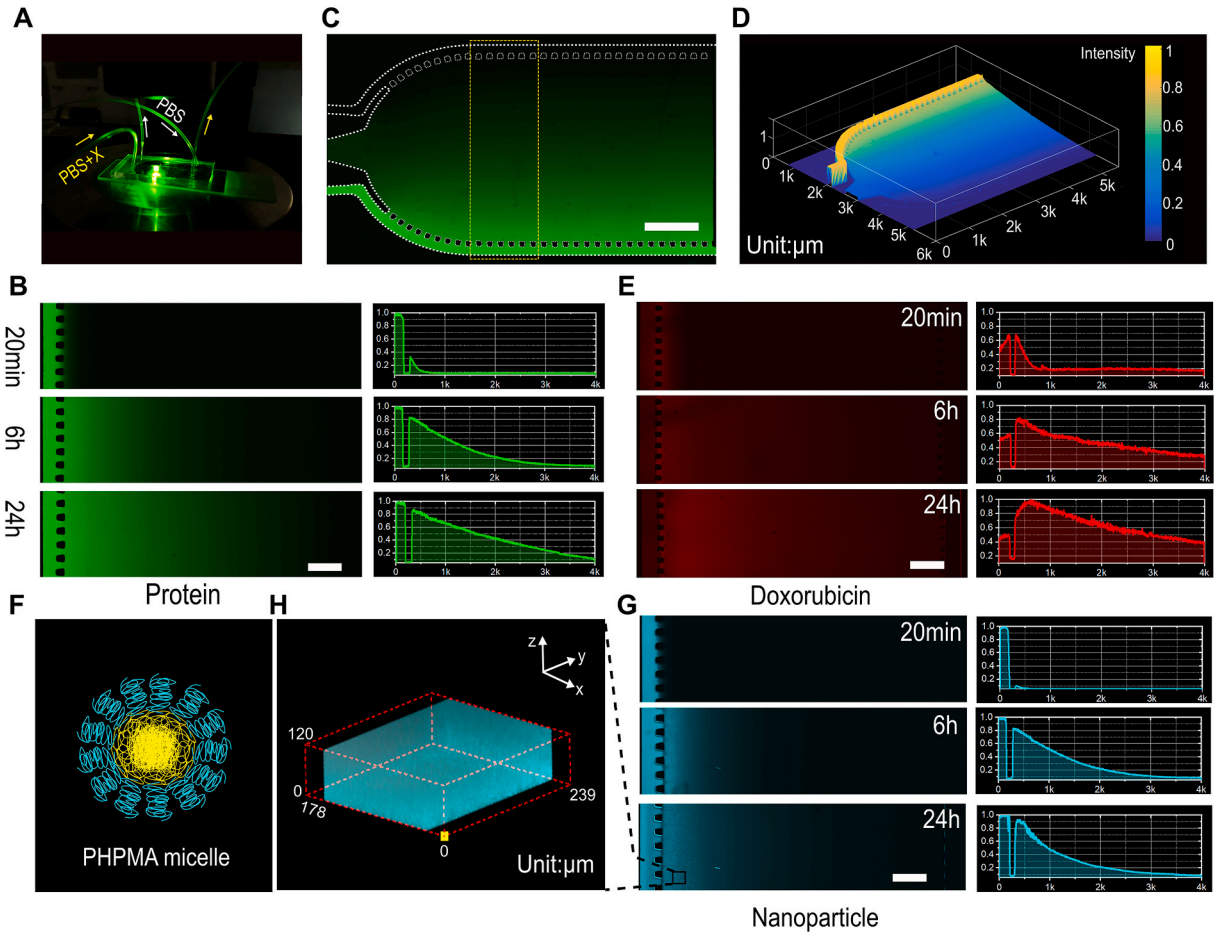

Fig. 2. Molecule diffusion on the chip. (A) Experimental setup under the confocal microscope. (B) Diffusion of antibody (immunoglobulin, large molecule) in the Matrigel on the chip. (C) Protein distribution in one chamber after 24h. (D) 3D illustration of the protein concentration in the chamber after 24h. (E) Doxorubicin (small molecule) distribution in the Matrigel on the chip. (F) Structure of the PHPMA micelle. (G) PHPMA micelles distribution in the Matrigel on the chip. (H) Enlarged 3D view of the distribution of PHPMA micelles in the Matrigel.

candidate. In this study, we studied the unidirectional communication between breast tumor cells and normal fibroblast. The cells were loaded into the chambers separately and cultured on the chip.

Here we co-cultured MRC-5 fibroblasts with invasive MDA-MB-231 or non-invasive MCF-7 breast tumor cells. After three days' co-culture, we measured the growth of tumor cells as well as the morphology and the expression of α -SMA of fibroblasts. The cells distributed evenly in the Matrigel after cell seeding (Fig. S3). As shown in Fig. 3A and B, during the culture, the influenced MDA-MB-231 formed more spheroids with a larger size, compared to the uninfluenced MDA-MB-231. This indicates that the secrets from the MRC-5 fibroblasts could increase the growth of the MDA-MB-231 cells even without direct contact. As shown in Fig. 3C and D, the MRC-5 fibroblasts also enhanced the growth of MCF-7 cells under unidirectional communication. The 3D profile of MDA-MB-231 and MCF-7 cells in the left chamber demonstrated that the MRC-5 fibroblasts enhanced the tumor growth, as shown in Fig. S4. We measured the size distribution of the spheroids (Fig. 3E), which shows that for the growth stimulation effects on MDA-MB-231 and MCF-7 by the fibroblasts was evident in most groups. Differently, the MDA-MB-231 cells formed fewer and smaller spheroids compared with MCF-7 cells. The control experiments were shown in Fig. S5 and Fig. S6. As shown in Fig. S5, the MDA-MB-231 or MCF-7 cells were seeded in one chamber. Another chamber was not seeded with any cells. The flow direction was set opposite. After three days' culture, it can be observed that the growth of the tumor cells on both sides had no obvious difference. In Fig. S6, the MDA-MB-231 or MCF-7 cells were seeded in one chamber. Another chamber was seeded with MRC-5 fibroblasts. The medium on both sides was set flowing from the MRC-5 to tumor cells. After three days' culture, it can be observed that the growth of the tumor cells on both sides had no obvious difference. Compared with Fig. S5, the density and size of tumor spheroids were promoted by MRC-5 fibroblasts. Together with Fig. 3, the results prove that the MRC-5 fibroblasts improved growth of tumor cells.

On the other hand, we observed high expression of α-SMA of MRC-5 fibroblast induced by the secrets of MDA-MB-231 cells (Fig. 3F and G). We quantified the expression of α-SMA by using the fluorescence ratio of α-SMA to cell nuclei (Fig. 3J) (Jeong et al., 2016). The ratio of the influenced fibroblasts was around 1.4-fold compared to the uninfluenced fibroblasts when co-cultured with the MDA-MB-231 (statistically different, $p < 0.01$). When co-cultured with the MCF-7, the MCR-5 fibroblasts showed no obvious difference in the expression of α-SMA, as shown in Fig. 3H and I. The ratios of α-SMA/cell nuclei on both sides were almost the same in the co-culture with the MCF-7 cells ($p > 0.05$). It indicates that the secreta of MDA-MB-231 cells could effectively turn the MRC-5 fibroblasts into CAFs, compared to the MCF-7 cells. Thus, it can be concluded that the transformation of normal fibroblasts into CAFs-like cells can be induced by tumor cells via unidirectional communication.

3.4. Unidirectional communication of MDA-MB-231 and MSCs

MSCs have been widely used as an important cell source for regenerative medicine due to the pluripotent differentiation, diverse sources, easy separation and amplification (Madl et al., 2018; Pittenger et al.,

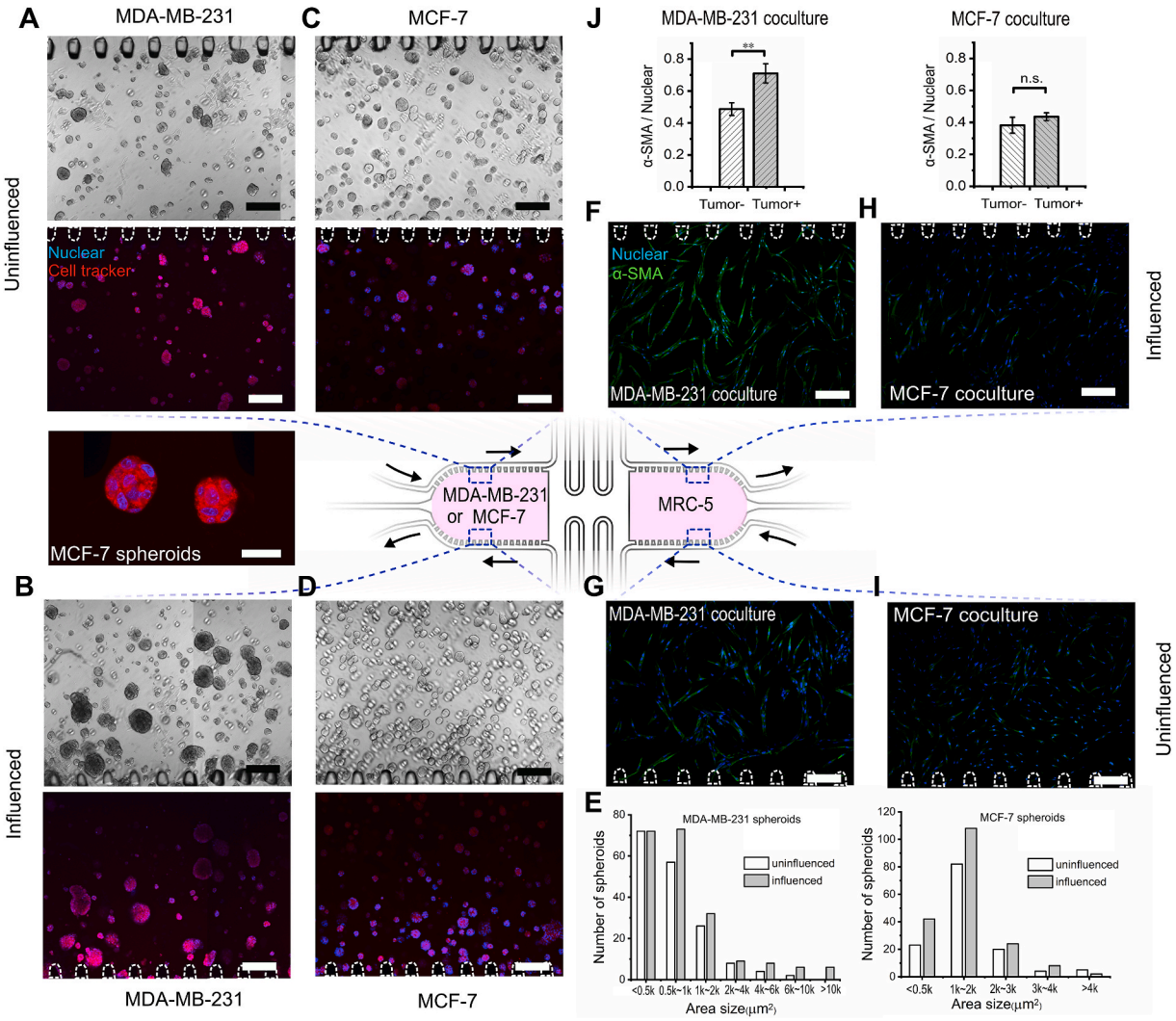

Fig. 3. Unidirectional communication between MRC-5 fibroblasts and MDA-MB-231 or MCF-7 cells. (A) MDA-MB-231 cells without the influence from MRC-5 fibroblasts. Upper and lower are the bright-field and fluorescent images, respectively. (B) MDA-MB-231 cells with the influence from MRC-5 fibroblasts. Upper and lower are the fluorescent and bright-field images, respectively (C) MCF-7 cells without the influence from MRC-5 fibroblasts. Upper and lower are the bright-field and fluorescent images. Scale bar: 200 μm. The insert is the MCF-7 spheroids under a 60 × objective lens. (D) MCF-7 cells with the influence from MRC-5 fibroblasts. (E) The number of MDA-MB-231 and MCF-7 spheroids with or without the influence from MRC-5 fibroblasts. (F) & (G) α-SMA expression of the MRC-5 fibroblasts influenced or uninfluenced by MDA-MB-231 cells, respectively. (H)&(I) α-SMA expression of the MRC-5 fibroblasts influenced or uninfluenced by MCF-7 cells, respectively. (J) The ratio of fluorescence of α-SMA to cell nuclei in MRC-5. Data present as means ± SD. **, statistical difference, $p < 0.01$. n.s., no statistical difference, $p > 0.05$. Scale bar = 50 μm (the insert) or 200 μm (the others).

1999). Moreover, MSCs display tropism to inflammation and malignant tumors and tend to migrate towards areas of wound healing or tumour growth (Cao et al., 2020; Kidd et al., 2009; Ruan et al., 2012; Valkenburg et al., 2018). So far, many studies have utilized MSCs to delivery drugs or nanomedicines into tumors, synergistic with chemotherapy, photothermal therapy, and photodynamic therapy for tumor theranostics (Cao et al., 2020; Ruan et al., 2012). As an essential type of tumor stromal cells, MSCs are also a top candidate of the CAFs (Shi et al., 2017). As shown in Fig. 4, we characterized both the tumor cells and MSCs after three days' unidirectional communication on the chip. The fluorescence and bright-field images of the MDA-MB-231 cells on the uninfluenced & influenced side were shown in Fig. 4A and 4B, respectively. It was found that the MDA-MB-231 proliferated faster and formed larger spheroid on the influenced side than did on the uninfluenced side; while the density of the spheroids was opposite. The tumor spheroids under a 60 × objective lens were also shown in the insert of Fig. 4. To better illustrate the difference, the 3D morphologies of the tumor spheroids on the two sides were analyzed, as illustrated in Fig. 4C. Although there were also many spheroids around the barriers on the uninfluenced side, the whole density of the spheroids was lower than that on the influenced side (Fig. 4C). The area size of the spheroids was analyzed by ImageJ and shown in Fig. 4D. The number of spheroids on the influenced side was higher than that on the uninfluenced side. The project area of some spheroids was even larger than 5k μm^2 affected by the secreta from MSCs. In addition, we co-cultured MSCs and MDA-MB-231 cells with the same flow direction (Fig. S7). The results show that the two sides of MDA-MB-231 cells influenced by MSCs showed no obvious difference, indicating that even normal MSCs have evident impacts on tumor cells.

Then we measured the expression of α-SMA in MSCs with immunofluorescent staining, as shown in Fig. 4E & G. Compared to the uninfluenced side, the influenced MSCs showed a brighter fluorescence, indicating a higher α-SMA expression. We also observed the changes in cell morphology. The MSCs with high α-SMA expression tend to show an elongated spindle shape, which is also observed in the bright-field images (Fig. 4F and H). To quantificate the fluorescence of α-SMA, we used the average fluorescence ratio of α-SMA to Hoechst 33342 stained cell

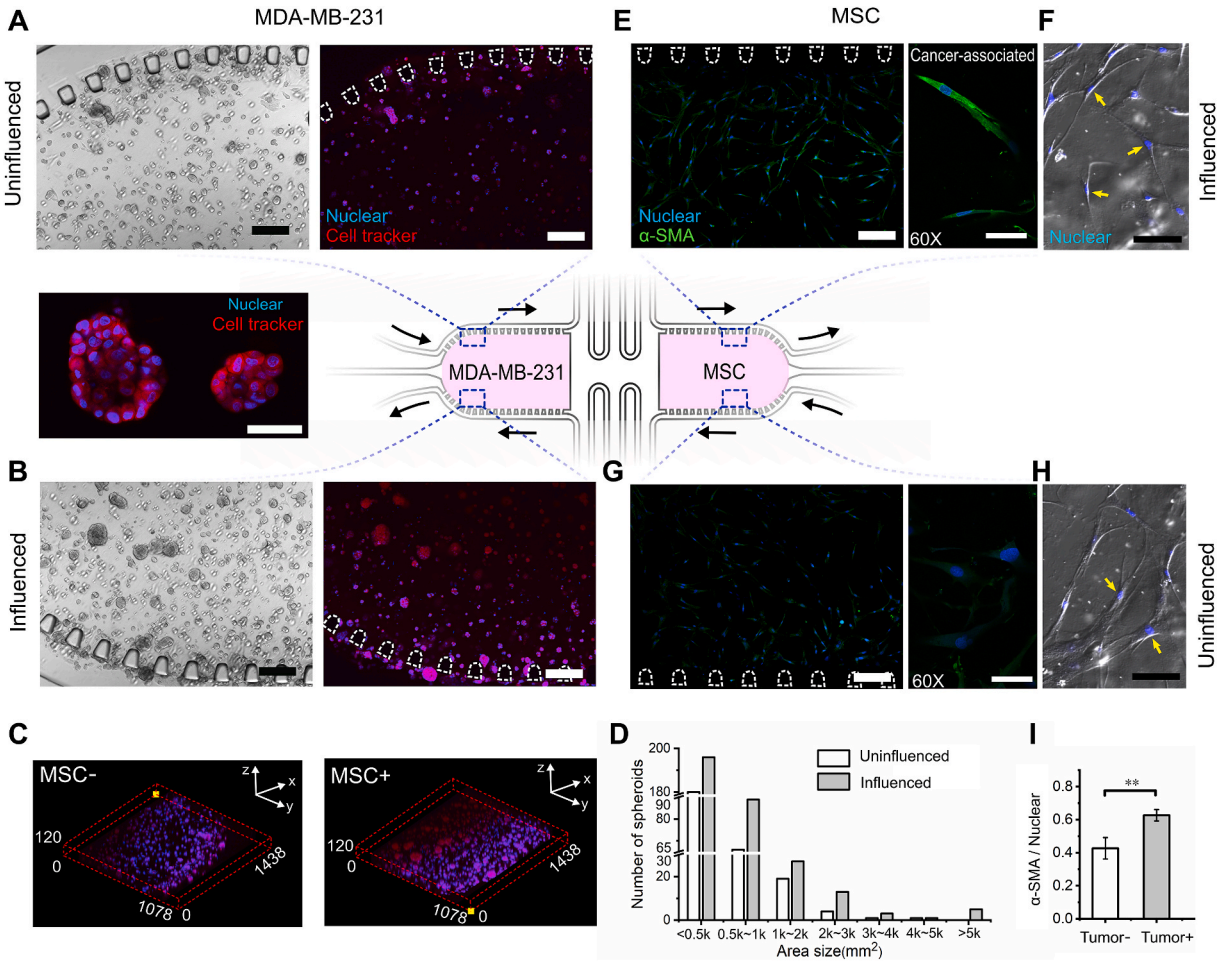

Fig. 4. Unidirectional communication between MSCs and MDA-MB-231 cells. (A) MDA-MB-231 cells without the influence from MSCs. Left and right are the bright-field and fluorescent images, respectively. Scale bar: 200 μm. Inset is the MDA-MB-231 breast tumor spheroids under a 60 × objective lens. Scale bar: 50 μm (B) MDA-MB-231 cells with the influence from MSCs. Scale bar: 200 μm. (C) 3D profile of the MDA-MB-231 cells without & with the influence from MSCs. (D) The number of spheroids without & with the influence from MSCs. (E) α-SMA expression of the influenced MSCs (scale bar: 200 μm) and the typical α-SMA expression under a 60 × objective lens (scale bar: 50 μm). (G) α-SMA expression of the influenced MSCs. Scale bar: 200 μm and the typical α-SMA expression under a 60 × objective lens. Scale bar: 50 μm. (F) & (H) Morphology of the typical MSC on the influenced side & on the uninfluenced side in the Matrigel. Scale bar: 50 μm. (I) Fluorescence ratio of α-SMA to cell nuclei. Data present as means ± SD. **, significant difference, $p < 0.01$.

nuclei (Fig. 4I). We found that the ratio of MSCs on the influenced side is around 1.5-fold higher than that on the uninfluenced side (statistically different, $p < 0.01$). We mono-cultured the MSCs on the chip as the control group (Fig. S8). It showed that the α-SMA fluorescence of mono-cultured MSCs was similar to that of uninfluenced MSCs. They did not present an apparent elongated shape. Thus, the secreted signal molecules of MDA-MB-231 cells up-regulated the expression of α-SMA, which indicates the induction of MSC to CAF-like cells even without direct contact. Both MSCs and MRC-5 fibroblasts are potential sources of CAFs in solid tumors.

3.5. TGF-β1 secreted from MAD-MB-231 cells induced MRC5 fibroblasts into CAFs

It has been reported that the TGF-β1 secreted by the tumor cells could induce fibroblasts transferring into CAFs (Calon et al., 2014). Here, we used the blocking channel to verify the role of TGF-β1 on this proposed chip. As shown in Fig. 5A, MDA-MB-231 cells and MRC-5 fibroblasts were seeded on the left and right chambers, respectively. The flow speed was set as 0.5 μL min^{-1} at each inlet. The antibody of TGF-β1 at a concentration of 10 ng mL^{-1} was introduced into the top blocking channel with the cell culture medium. The flow speed was set as 0.5 μL min^{-1}, which ensures around 20 min for the neutralization of TFG- β1 with the antibody before it reached the fibroblast culture chamber. Medium with the antibody was introduced into the bottom blocking channel as a control. As shown in Fig. 5B, we hypothesized that if the TGF-β1 was blocked by the antibody, it could not transfer MCR-5 into CAF-like cells. After three days' culture, we found that the expression of α-SMA of the influenced MRC-5 was not statistically different from the uninfluenced MRC-5 (bottom area) Fig. 5C and D. The ratio of α-SMA/Nuclei was 0.42 ± 0.02 was also much lower than the ratio of unblocked MRC-5 cells at 0.71 ± 0.06 in Fig. 3E. These results indicate that the TGF-β1 secreted by the tumor cells is one of the driven forces to turn the normal fibroblasts into CAFs. The blocking channels on the chip functioned adequately, which could simplify the biological experiments and reduce the system errors.

4. Discussion

Microfluidic devices have been attracting more attention from biomedical researchers (Saini et al., 2020; Truong et al., 2019a; Xu et al., 2013). The microfluidic chips enable real-time monitoring, provide excellent visualization, reduce sample and reagent usage, control the chemical concentration gradients, and enhance cell responses through restrained culture space, which could reduce the consumption of cells, medium and some expensive agents. Many microfluidic devices have

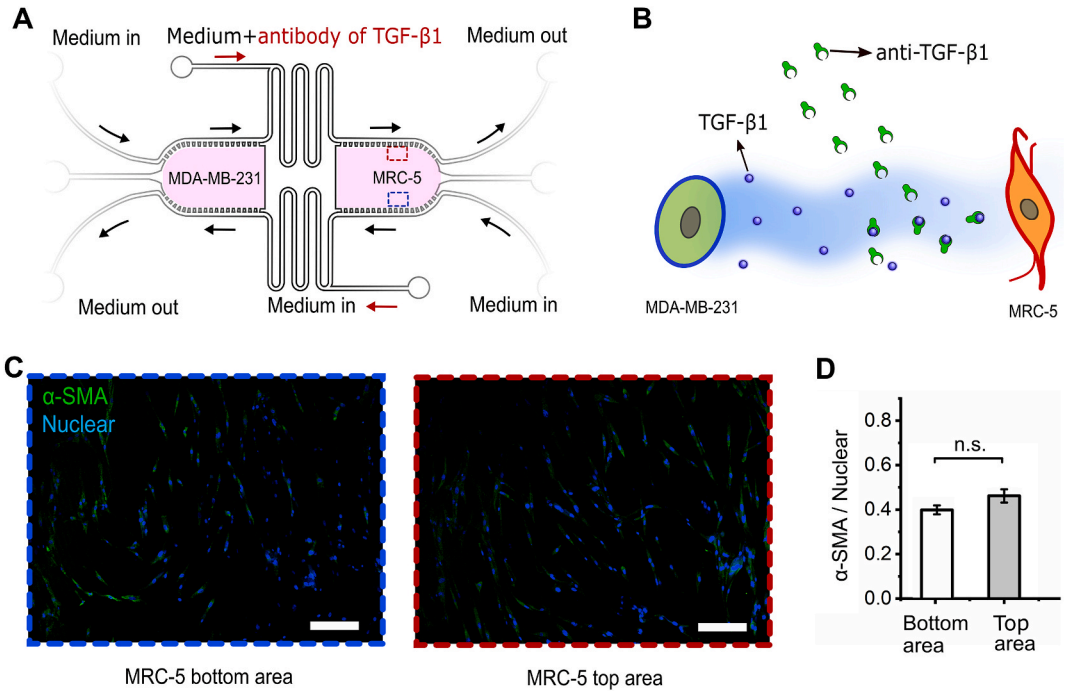

Fig. 5. Injection of TGF-β1 antibodies through the blocking channel ceased the transformation of MCR-5 fibroblasts into CAFs-like cells. (A) The setup of using signal blocking inlet on the chip to study the effects of TGF-β1. (B) The schematic of using the antibody of TGF-β1 to block its function to MRC-5. (C) α-SMA expression of the MRC-5 on the bottom area (Left, without the influence from MDA-MB-231 cells) and on the top area (Right, with the influence from MDA-MB-231 cell with the TGF-β1 antibody). (D) Fluorescence ratio of α-SMA to nuclei of MRC-5 cells in the right chamber. Data present as means ± SD. n.s., no statistical difference, $p > 0.05$.

been used to study intercellular communications (Alonzo et al., 2015; Zheng et al., 2017), especially between tumor cells and stromal cells (Chen et al., 2016). For example, Rahman *et al.* evaluated intercellular communication between breast cancer cells and adipose-derived stem cells via passive diffusion in a two-layer microfluidic device (Rahman et al., 2020). A similar design was utilized to study the interactions between A549 lung cancer cells and vascular endothelial cells during treatment with exosome encapsulating microRNA (Jeong et al., 2020). Under 3D microenvironment, the cells in 3D can better reflect the reality of cells in the body (Jun et al., 2019). Seok *et al.* fabricated three on-chip channels which were connected by collagen scaffolds (Chung et al., 2009). One cell type was seeded in the middle channel, and the medium or the other types of cells were introduced into the side channels. Fang et al. investigated the communication of tumor cells with fibroblasts and vascular endothelial cells in gradient-sized 3D spheroids on agarose chips (Fang et al., 2019). Truong *et al.* developed a 3D organotypic microfluidic platform, integrated with hydrogel-based biomaterials, to mimic the vascular niche of glioma stem cells and study the influence of endothelial cells on patient-derived glioma stem cells and identify signaling cues that mediate their invasion and phenotype (Truong et al., 2019a). Furthermore, other methods were proposed using the microfluidic such as the droplet co-culture (Chen et al., 2014; Du et al., 2018; Park et al., 2011; Tomasi et al., 2020), micro-Boden chamber (Karakas et al., 2017), and communication in single-cell level (Karakas et al., 2017). However, the above reported methods co-culture the cells without considering the direction of signal transfer. In this work we provide a new approach of cell co-culture with unidirectional transfer of signal molecules to clear the details of the intercellular communication. The special design could control the signal direction and provide a 3D microenvironment for cells to study the Signal-Target-Response pathway.

The tumor microenvironment composed of stromal cells and the extracellular matrix (ECM) has crucial roles in tumorigenesis, tumor progression, metastasis, and therapy resistance (Valkenburg et al., 2018). Moreover, tumor cells can influence the stromal cells and modify the ECM generating a favorable niche that facilitates tumor progression (Calon et al., 2014; Shi et al., 2017). Both MDA-MB-231 and MCF-7 cells are breast cancer cell lines. They displayed distinct capacities to turn normal fibroblasts into myofibroblast-like cells. The MRC-5 fibroblasts demonstrated up-regulated α-SMA expression induced by MDA-MB-231 cells other than MCF-7 cells. In breast cancer, TGF-β1 is highly expressed, especially at the advancing edges of primary tumors and in metastatic foci of lymph nodes (Dalal et al., 1993). It has been reported that the more invasive MDA-MB-231 cells produced five times more TGF-β1 than the less invasive MCF-7 line when cultured *in vitro* with 10% serum plus DMEM/F12 (Guerrero et al., 2010). It indicates that TGF-β1 plays an important role to influence the neighboring stromal cells. The fibroblasts influence the behaviors of tumor cells via a range of growth factors and cytokines including HGF, EFG, BMPs, interleukins, and even lactate products (Kalluri 2016; Sahai et al., 2020; Shi et al., 2017). It is difficult to identify a specific inhibitor that can block the function of the complicated secret from fibroblasts. On the other hand, TGF-β1 has been proven as one of the major factors to transfer fibroblasts into CAFs (Calon et al., 2014; Ringuette Goulet et al., 2018). Our results in Fig. 5 show the blocking of TGF-β1 can stop the transformation of CAFs as well as demonstrated the blocking function of the unidirectional chip.

Previous studies have demonstrated that mesenchymal stem/stromal cells contribute to direct interaction with tumor cells and promote mutual exchange/induction of cellular markers (Karnoub et al., 2007; Shi et al., 2017). Alternatively, MSC interaction can be mediated indirectly by the release of soluble biological factors and/or vesicles such as exosomes whereby MSC can affect cellular functionality of distant cell populations in a paracrine manner. The signal molecules secreted by the tumor cells can also influence the targeting, migration and functions of MSCs. These effects can be mediated both, by signal proteins such as CXCL12-CXCR4 and CCL19-CCR7(Ruan et al., 2012), and RNAs including mRNAs and miRNAs (Hergenreider et al., 2012; Jeong et al., 2020). It has been reported that the proliferation and migration of cancer cells increased following direct co-culture with MSCs. These

results suggest that MSCs induce epithelial mesenchymal transition in cancer cells via direct cell-to-cell contact and may play an essential role in cancer metastasis (Takigawa et al., 2017). In this work, we found that unidirectional indirect contact can trigger the response of cancer cells and CAFs, which may be due to the high bioactivities of signal molecules in the chip without a decrease in conditioned medium storage and transferring.

The unidirectional microfluidic chips have high extensibility that is applicable for different research, such as exosome or endocrine studies (Fig. S9). Exosomes are known for intercellular communication in both normal and diseased tissue. They are involved in the regulation of programmed cell death, modulation of the immune response, inflammation, angiogenesis, and coagulation (Dourado et al., 2019; Hergenreider et al., 2012; Huang et al., 2020). The exosomes secreted by stromal cells, such as MSCs, have been demonstrated to alter tumor cellular functionalities with the capacity to reconstruct tumor microenvironment (Yang et al., 2015). It has been reported that cancer cells induce CAFs through TGF-β1 encapsulated exosomes (Ringuette Goulet et al., 2018). Cancer exosomes trigger MSC differentiation into pro-angiogenic and pro-invasive myofibroblasts (Chowdhury et al., 2015). Injection of antibodies to block the exosomes may be used to study the functions of a specific type of exosomes. Opening an outlet in the middle channel can provide an exosome harvesting path or a connection path to other microfluidic devices for monitoring of exosomes. Microfluidics-based separation and detection of exosomes have attracted more attentions for research and clinical applications (Lin et al., 2020; Zhang et al., 2019). It is expected that the proposed unidirectional microfluidic chip can be extend with the chips for separation and detection of exosomes, which may provide an efficient approach for exosome studies. Our unidirectional microfluidic device may also be used in endocrine studies. By optimizing the middle channel length and introducing endothelial cell culture in the channels and physical barriers, the unidirectional chip may be a simple model that mimics the in vivo endocrine transfer pathway.

5. Conclusions

In this work, a microfluidic chip was fabricated for cell co-culture to study the unidirectional intercellular communication. The chip achieved unidirectional communication of 3D cultured cells. Moreover, the unidirectional chip enables the analysis of a specific signal via the signal-blocking inlet. Our results showed that MRC-5 and MSCs could enhance the growth of cancer cells. The invasive MDA-MB-231 could more effectively induce the MRC-5 and MSCs into CAF-like cells via unidirectional stimulation. By using the signal-blocking function, we also proved that TGF-β1 secreted by cells was one of the major factors to up-regulate the expression of α-SMA of the stromal cells. The device offers a unique, facial and effective tool for the study of intercellular communication.

CRediT authorship contribution statement

Guocheng Fang: Writing - original draft, conceived of the presented idea, carried out the experiments, and wrote the manuscript. **Hongxu Lu:** Writing - original draft, Supervision, conceived of the presented idea, carried out the experiments, and wrote the manuscript, supervised the project. **Hamidreza Aboulkheyr Es:** helped the cancer assosicted fibroblast characterisation and microfluidic design. **Dejiang Wang:** assisted the cell culture and microfluidic design. **Yuan Liu:** assisted the cell culture and microfluidic design. **Majid Ebrahimi Warkiani:** helped the cancer assosicted fibroblast characterisation and microfluidic design. **Gungun Lin:** assisted the cell culture and microfluidic design. **Dayong Jin:** Supervision, supervised the project. All authors discussed the results and contributed to the final manuscript.

Declaration of competing interest

The authors declare that they have no known competing financial interests or personal relationships that could have appeared to influence the work reported in this paper.

Acknowledgements

The authors acknowledge the financial support from the China Scholarship Council (G.C. Fang: No. 201708140082. Y. Liu: No.201608140100; D.J. Wang: No 201706170027), the National Health and Medical Research Council (NHMRC) (GNT1160635), ARC Industry Transformational Research Hub Scheme (IH150100028), ARC Linkage Infrastructure, Equipment and Facilities (LIEF) Project (LE180100043), Australia-China Joint Research Centre for Point-of-Care Testing (ACSRF65827, SQ2017YFGH001190), Science and Technology Innovation Commission of Shenzhen (KQTD20170810110913065), and National Natural Science Foundation of China (NSFC, 61729501, 51720105015).

Appendix A. Supplementary data

Supplementary data to this article can be found online at https://doi.org/10.1016/j.bios.2020.112833.

References

Aboulkheyr Es, H., Zhand, S., Thiery, J.P., Warkiani, M.E., 2020. Pirfenidone reduces immune-suppressive capacity of cancer-associated fibroblasts through targeting CCL17 and TNF-beta. Integr. Biol. 12 (7), 188–197.
Alberts, B., Johnson, A., Lewis, J., Raff, M., Roberts, K., Walter, P., 2002. Molecular Biology of the Cell, fourth ed. Garland Science.
Alonzo, L.F., Moya, M.L., Shirure, V.S., George, S.C., 2015. Microfluidic device to control interstitial flow-mediated homotypic and heterotypic cellular communication. Lab Chip 15 (17), 3521–3529.
Bogdanowicz, D.R., Lu, H.H., 2013. Studying cell-cell communication in co-culture. Biotechnol. J. 8 (4), 395–396.
Calon, A., Tauriello, D.V.F., Batlle, E., 2014. TGF-beta in CAF-mediated tumor growth and metastasis. Semin. Cancer Biol. 25, 15–22.
Cao, W., Liu, B., Xia, F., Duan, M., Hong, Y., Niu, J., Wang, L., Liu, Y., Li, C., Cui, D., 2020. MnO_2@Ce6-loaded mesenchymal stem cells as an "oxygen-laden guided-missile" for the enhanced photodynamic therapy on lung cancer. Nanoscale 12 (5), 3090–3102.
Chen, Y.C., Zhang, Z., Fouladdel, S., Deol, Y., Ingram, P.N., McDermott, S.P., Azizi, E., Wicha, M.S., Yoon, E., 2016. Single cell dual adherent-suspension co-culture microenvironment for studying tumor–stromal interactions with functionally selected cancer stem-like cells. Lab Chip 16 (15), 2935–2945.
Chen, Y.C., Cheng, Y.H., Kim, H.S., Ingram, P.N., Nor, J.E., Yoon, E., 2014. Paired single cell co-culture microenvironments isolated by two-phase flow with continuous nutrient renewal. Lab Chip 14 (16), 2941–2947.
Chowdhury, R., Webber, J.P., Gurney, M., Mason, M.D., Tabi, Z., Clayton, A., 2015. Cancer exosomes trigger mesenchymal stem cell differentiation into pro-angiogenic and pro-invasive myofibroblasts. Oncotarget 6 (2), 715–731.
Chung, S., Sudo, R., Mack, P.J., Wan, C.-R., Vickerman, V., Kamm, R.D., 2009. Cell migration into scaffolds under co-culture conditions in a microfluidic platform. Lab Chip 9 (2), 269–275.
Cirri, P., Chiarugi, P., 2011. Cancer associated fibroblasts: the dark side of the coin. Am. J Cancer Res. 1 (4), 482–497.
Dalal, B.I., Keown, P.A., Greenberg, A.H., 1993. Immunocytochemical localization of secreted transforming growth factor-beta 1 to the advancing edges of primary tumors and to lymph node metastases of human mammary carcinoma. Am. J. Pathol. 143 (2), 381–389.
Dorayappan, K.D.P., Gardner, M.L., Hisey, C.L., Zingarelli, R.A., Smith, B.Q., Lightfoot, M.D.S., Gogna, R., Flannery, M.M., Hays, J., Hansford, D.J., Freitas, M.A., Yu, L., Cohn, D.E., Selvendiran, K., 2019. A microfluidic chip enables isolation of exosomes and establishment of their protein profiles and associated signaling pathways in ovarian cancer. Canc. Res. 79 (12), 3503–3513.
Dourado, M.R., Korvala, J., Åström, P., De Oliveira, C.E., Cervigne, N.K., Mofatto, L.S., Campanella Bastos, D., Pereira Messetti, A.C., Graner, E., Paes Leme, A.F., Coletta, R. D., Salo, T., 2019. Extracellular vesicles derived from cancer-associated fibroblasts induce the migration and invasion of oral squamous cell carcinoma. J. Extracell. Vesicles 8 (1), 1578525.
Du, X., Li, W., Du, G., Cho, H., Yu, M., Fang, Q., Lee, L.P., Fang, J., 2018. Droplet array-based 3D coculture system for high-throughput tumor angiogenesis assay. Anal. Chem. 90 (5), 3253–3261.
Fang, G., Lu, H., Law, A., Gallego-Ortega, D., Jin, D., Lin, G., 2019. Gradient-sized control of tumor spheroids on a single chip. Lab Chip 19 (24), 4093–4103.

Guerrero, J., Tobar, N., Cáceres, M., Espinoza, L., Escobar, P., Dotor, J., Smith, P.C., Martínez, J., 2010. Soluble factors derived from tumor mammary cell lines induce a stromal mammary adipose reversion in human and mice adipose cells. Possible role of TGF-beta1 and TNF-alpha. Breast Cancer Res. Treat. 119 (2), 497–508.
Hergenreider, E., Heydt, S., Tréguer, K., Boettger, T., Horrevoets, A.J.G., Zeiher, A.M., Scheffer, M.P., Frangakis, A.S., Yin, X., Mayr, M., Braun, T., Urbich, C., Boon, R.A., Dimmeler, S., 2012. Atheroprotective communication between endothelial cells and smooth muscle cells through miRNAs. Nat. Cell Biol. 14 (3), 249–256.
Huang, G., Lin, G., Zhu, Y., Duan, W., Jin, D., 2020. Emerging technologies for profiling extracellular vesicle heterogeneity. Lab Chip 20 (14), 2423–2437.
Jeong, K., Yu, Y.J., You, J.Y., Rhee, W.J., Kim, J.A., 2020. Exosome-mediated microRNA-497 delivery for anti-cancer therapy in a microfluidic 3D lung cancer model. Lab Chip 20 (3), 548–557.
Jeong, S.Y., Lee, J.H., Shin, Y., Chung, S., Kuh, H.J., 2016. Co-culture of tumor spheroids and fibroblasts in a collagen matrix-incorporated microfluidic chip mimics reciprocal activation in solid tumor microenvironment. PloS One 11 (7), e0159013.
Jiang, H., Jiang, D., Zhu, P., Pi, F., Ji, J., Sun, C., Sun, J., Sun, X., 2016. A novel mast cell co-culture microfluidic chip for the electrochemical evaluation of food allergen. Biosens. Bioelectron. 83, 126–133.
Jun, Y., Lee, J., Choi, S., Yang, J.H., Sander, M., Chung, S., Lee, S.-H., 2019. In vivo–mimicking microfluidic perfusion culture of pancreatic islet spheroids. Sci. Adv. 5 (11), eaax4520.
Kalluri, R., 2016. The biology and function of fibroblasts in cancer. Nat. Rev. Canc. 16 (9), 582–598.
Kalluri, R., Zeisberg, M., 2006. Fibroblasts in cancer. Nat. Rev. Canc. 6 (5), 392–401.
Karakas, H.E., Kim, J., Park, J., Oh, J.M., Choi, Y., Gozuacik, D., Cho, Y.K., 2017. A microfluidic chip for screening individual cancer cells via eavesdropping on autophagy-inducing crosstalk in the stroma niche. Sci. Rep. 7 (1), 2050.
Karnoub, A.E., Dash, A.B., Vo, A.P., Sullivan, A., Brooks, M.W., Bell, G.W., Richardson, A. L., Polyak, K., Tubo, R., Weinberg, R.A., 2007. Mesenchymal stem cells within tumour stroma promote breast cancer metastasis. Nature 449 (7162), 557–563.
Kholodenko, B.N., 2006. Cell-signalling dynamics in time and space. Nature Rev. Mol. Cell Biol. 7 (3), 165–176.
Kidd, S., Spaeth, E., Dembinski, J.L., Dietrich, M., Watson, K., Klopp, A., Battula, V.L., Weil, M., Andreeff, M., Marini, F.C., 2009. Direct evidence of mesenchymal stem cell tropism for tumor and wounding microenvironments using in vivo bioluminescent imaging. Stem Cell. 27 (10), 2614–2623.
Lee, S.W., Kwak, H.S., Kang, M.-H., Park, Y.-Y., Jeong, G.S., 2018. Fibroblast-associated tumour microenvironment induces vascular structure-networked tumouroid. Sci. Rep. 8 (1), 2365.
Lin, S., Yu, Z., Chen, D., Wang, Z., Miao, J., Li, Q., Zhang, D., Song, J., Cui, D., 2020. Progress in microfluidics-based exosome separation and detection technologies for diagnostic applications. Small 16 (9), 1903916.
Lin, S., Zhi, X., Chen, D., Xia, F., Shen, Y., Niu, J., Huang, S., Song, J., Miao, J., Cui, D., Ding, X., 2019. A flyover style microfluidic chip for highly purified magnetic cell separation. Biosens. Bioelectron. 129, 175–181.
Lu, H., Utama, R.H., Kitiyotsawat, U., Babiuch, K., Jiang, Y., Stenzel, M.H., 2015. Enhanced transcellular penetration and drug delivery by crosslinked polymeric micelles into pancreatic multicellular tumor spheroids. Biomater. Sci. 3 (7), 1085–1095.
Madl, C.M., Heilshorn, S.C., Blau, H.M., 2018. Bioengineering strategies to accelerate stem cell therapeutics. Nature 557 (7705), 335–342.
Mitra, A.K., Zillhardt, M., Hua, Y., Tiwari, P., Murmann, A.E., Peter, M.E., Lengyel, E., 2012. MicroRNAs reprogram normal fibroblasts into cancer-associated fibroblasts in ovarian cancer. Canc. Discov. 2 (12), 1100–1108.
Moutinho Jr., T.J., Panagides, J.C., Biggs, M.B., Medlock, G.L., Kolling, G.L., Papin, J.A., 2017. Novel co-culture plate enables growth dynamic-based assessment of contact-independent microbial interactions. PloS One 12 (8), e0182163.
Neitzel, J., Rasband, M.. Cell communication. https://www.nature.com/scitable/topic/cell-communication-14122659/.
Park, J., Kerner, A., Burns, M.A., Lin, X.N., 2011. Microdroplet-enabled highly parallel co-cultivation of microbial communities. PloS One 6 (2), e17019.
Pittenger, M.F., Mackay, A.M., Beck, S.C., Jaiswal, R.K., Douglas, R., Mosca, J.D., Moorman, M.A., Simonetti, D.W., Craig, S., Marshak, D.R., 1999. Multilineage potential of adult human mesenchymal stem cells. Science 284 (5411), 143–147.
Rahman, S.M., Campbell, J.M., Coates, R.N., Render, K.M., Byrne, C.E., Martin, E.C., Melvin, A.T., 2020. Evaluation of intercellular communication between breast cancer cells and adipose-derived stem cells via passive diffusion in a two-layer microfluidic device. Lab Chip 20 (11), 2009–2019.
Ringuette Goulet, C., Bernard, G., Tremblay, S., Chabaud, S., Bolduc, S., Pouliot, F., 2018. Exosomes induce fibroblast differentiation into cancer-associated fibroblasts through TGFbeta signaling. Mol. Cancer Res. 16 (7), 1196–1204.
Ruan, J., Ji, J., Song, H., Qian, Q., Wang, K., Wang, C., Cui, D., 2012. Fluorescent magnetic nanoparticle-labeled mesenchymal stem cells for targeted imaging and hyperthermia therapy of in vivo gastric cancer. Nanoscale Res. Lett. 7 (1), 309.
Sahai, E., Astsaturov, I., Cukierman, E., DeNardo, D.G., Egeblad, M., Evans, R.M., Fearon, D., Greten, F.R., Hingorani, S.R., Hunter, T., Hynes, R.O., Jain, R.K., Janowitz, T., Jorgensen, C., Kimmelman, A.C., Kolonin, M.G., Maki, R.G., Powers, R. S., Puré, E., Ramirez, D.C., Scherz-Shouval, R., Sherman, M.H., Stewart, S., Tlsty, T. D., Tuveson, D.A., Watt, F.M., Weaver, V., Weeraratna, A.T., Werb, Z., 2020. A framework for advancing our understanding of cancer-associated fibroblasts. Nat. Rev. Canc. 20 (3), 174–186.
Saini, H., Rahmani Eliato, K., Veldhuizen, J., Zare, A., Allam, M., Silva, C., Kratz, A., Truong, D., Mouneimne, G., LaBaer, J., Ros, R., Nikkhah, M., 2020. The role of tumor-stroma interactions on desmoplasia and tumorigenicity within a microengineered 3D platform. Biomaterials 247, 119975.
Shi, Y., Du, L., Lin, L., Wang, Y., 2017. Tumour-associated mesenchymal stem/stromal cells: emerging therapeutic targets. Nature Rev. Drug Discov. 16 (1), 35–52.
Shim, S., Belanger, M.C., Harris, A.R., Munson, J.M., Pompano, R.R., 2019. Two-way communication between ex vivo tissues on a microfluidic chip: application to tumor–lymph node interaction. Lab Chip 19 (6), 1013–1026.
Shimasaki, T., Yamamoto, S., Arisawa, T., 2018. Exosome research and co-culture study. Biol. Pharm. Bull. 41 (9), 1311–1321.
Shimoda, M., Mellody, K.T., Orimo, A., 2010. Carcinoma-associated fibroblasts are a rate-limiting determinant for tumour progression. Semin. Cell Dev. Biol. 21 (1), 19–25.
Takigawa, H., Kitadai, Y., Shinagawa, K., Yuge, R., Higashi, Y., Tanaka, S., Yasui, W., Chayama, K., 2017. Mesenchymal stem cells induce epithelial to mesenchymal transition in colon cancer cells through direct cell-to-cell contact. Neoplasia 19 (5), 429–438.
Telleen, S., 2018. Human Physiology Part 1: Foundation Concepts (OpenStax CNX).
Tomasi, R.F.X., Sart, S., Champetier, T., Baroud, C.N., 2020. Individual control and quantification of 3D spheroids in a high-density microfluidic droplet array. Cell Rep. 31 (8), 107670.
Truong, D., Fiorelli, R., Barrientos, E.S., Melendez, E.L., Sanai, N., Mehta, S., Nikkhah, M., 2019a. A three-dimensional (3D) organotypic microfluidic model for glioma stem cells – vascular interactions. Biomaterials 198, 63–77.
Truong, D.D., Kratz, A., Park, J.G., Barrientos, E.S., Saini, H., Nguyen, T., Pockaj, B., Mouneimne, G., LaBaer, J., Nikkhah, M., 2019b. A human organotypic microfluidic tumor model permits investigation of the interplay between patient-derived fibroblasts and breast cancer cells. Canc. Res. 79 (12), 3139–3151.
Valkenburg, K.C., de Groot, A.E., Pienta, K.J., 2018. Targeting the tumour stroma to improve cancer therapy. Nature Rev. Clin. Oncol. 15 (6), 366–381.
Vu, T.Q., de Castro, R.M.B., Qin, L., 2017. Bridging the gap: microfluidic devices for short and long distance cell–cell communication. Lab Chip 17 (6), 1009–1023.
Xu, Z., Gao, Y., Hao, Y., Li, E., Wang, Y., Zhang, J., Wang, W., Gao, Z., Wang, Q., 2013. Application of a microfluidic chip-based 3D co-culture to test drug sensitivity for individualized treatment of lung cancer. Biomaterials 34 (16), 4109–4117.
Yang, Y., Bucan, V., Baehre, H., von der Ohe, J., Otte, A., Hass, R., 2015. Acquisition of new tumor cell properties by MSC-derived exosomes. Int. J. Oncol. 47 (1), 244–252.
Yu, J., Berthier, E., Craig, A., de Groot, T.E., Sparks, S., Ingram, P.N., Jarrard, D.F., Huang, W., Beebe, D.J., Theberge, A.B., 2019. Reconfigurable open microfluidics for studying the spatiotemporal dynamics of paracrine signalling. Nature Biomed Eng 3 (10), 830–841.
Zervantonakis, I.K., Hughes-Alford, S.K., Charest, J.L., Condeelis, J.S., Gertler, F.B., Kamm, R.D., 2012. Three-dimensional microfluidic model for tumor cell intravasation and endothelial barrier function. Proc. Natl. Acad. Sci. U.S.A. 109 (34), 13515–13520.
Zhang, P., Zhou, X., He, M., Shang, Y., Tetlow, A.L., Godwin, A.K., Zeng, Y., 2019. Ultrasensitive detection of circulating exosomes with a 3D-nanopatterned microfluidic chip. Nature Biomed. Eng. 3 (6), 438–451.
Zheng, Y., Wang, S., Xue, X., Xu, A., Liao, W., Deng, A., Dai, G., Liu, A.P., Fu, J., 2017. Notch signaling in regulating angiogenesis in a 3D biomimetic environment. Lab Chip 17 (11), 1948–1959.